

学位論文

「Serum anti-Gal-3 autoantibody is a predictive marker of the efficacy of platinum-based chemotherapy in against pulmonary adenocarcinoma.」

（血清抗 Gal-3 自己抗体は肺腺癌に対するプラチナ製剤を基本とした
化学療法の効果予測マーカーである。）

DM 12026 柳田 憲吾

北里大学大学院医療系研究科医学専攻博士課程
生体構造医科学群 応用腫瘍病理
指導教授 佐藤 雄一

著者の宣言

本学位論文は、著者の責任において実験を遂行し、得られた真実の結果に基づいて正確に作成したものに相違ないことをここに宣言する。

目的

肺腺癌の化学療法はALKやEGFRなどの遺伝子変異に対する分子標的薬治療が広く行われているが、これらの遺伝子変異のある肺腺癌患者は全体の約35%である。これらの分子標的薬は遺伝子変異のない肺腺癌患者には奏効性がないため、多くの患者はプラチナ製剤を基本とした多剤併用療法が主に用いられている。プラチナ製剤は遺伝子変異の有無に関わらず高い治療効果があるため、一次、二次治療薬として用いられることが多い。しかし、副作用が強く、奏効率も20%程度であり、事前に治療効果が期待できないことが予測できれば、非プラチナ製剤を用いた治療に変更することも可能となる。

本研究では、プラチナ製剤感受性予測マーカーの獲得を目指し、プラチナ製剤を用いた治療を受け、その治療効果判定が既知である肺腺癌患者の治療前血清を一次抗体とした二次元免疫ブロット法を行い、自己抗体利用したプラチナ製剤治療感受性予測マーカー探索を網羅的に行った。

方法

材料：プラチナ製剤を基本とした多剤併用療法を行い、RECISTによる治療の効果判定が既知である肺腺癌患者の治療前に採血した血清(治療前血清)と、同じく治療前に採取した腫瘍の生検組織(治療前腫瘍組織)を用いた。

二次元免疫ブロット法：シスプラチン耐性にした肺腺癌細胞株(シスプラチン耐性株)からタンパク質を抽出し、二次元電気泳動法にて展開した。PVDF膜に転写後、化学療法で奏効群または進行群と判断されたそれぞれ3例の治療前混合血清を一次抗体に用いた免疫ブロット法を行い、それぞれで自己抗体が認識する抗原タンパク質を検出した。その後、CBB染色したゲルから自己抗体が認識した抗原スポットを切り出し、トリプシンを用いたゲル内消化後、質量分析装置にて抗原タンパク質を同定した。

Dot Blot 解析：シスプラチン耐性株から抽出したタンパク質を二次元電気泳動法にて展開後、目的とする Galectin-3 (Gal-3)のスポットをゲルから切り出し、Electro Elution法にてタンパク質を抽出した。抽出したタンパク質を抗原とした Dot Blot 法により、22症例の治療前血清中の自己抗体量を測定した。その後、シグナル解析ソフトウェアを用いて進行群を判別群、奏効/安定群を対照群とした ROC 解析を行った。

免疫染色法：10%ホルマリン固定パラフィン包埋された40例の治療前腫瘍生検組織を対象に、一次抗体に抗 Gal-3 抗体を用いて免疫染色を行った。腫瘍細胞の細胞質に明らかな発現が認められたものを陽性、認められなかったものを陰性と評価した。

結果

治療前血清を一次抗体とした二次元免疫ブロット法(図1)により自己抗体が認識する抗原タンパク質は進行群で51種、奏効群で12種が同定された。今回、進行群のみで検出され、薬剤感受性との関連性が多く報告されている Gal-3 に着目し、さらに検討を進めた。

22例の肺腺癌患者の治療前血清中の抗 Gal-3 自己抗体量を Dot Blot 解析により測定した結果、奏効/安定群に比して進行群で有意に抗 Gal-3 自己抗体量が増加していた($p =$

0.0084, 図 2)。Receiver operating characteristic curve (ROC)解析では進行群を判別群、奏効/安定群を対照群とした場合、The area under the curve (AUC)が 0.84 であり、最適 Cut off 値を 1,086 と設定した時、感度が 67%、特異度が 92%で両者を鑑別可能であった。

また、肺腺癌患者の治療前腫瘍組織を用いた免疫染色の結果、Gal-3 の発現は進行群では 15 例中 10 例(66.7%)、安定群では 14 例中 7 例(50.0%)、奏効群では 11 例 2 例(18.2%)と徐々に陽性率が低下していた(図 3)。また、Gal-3 タンパク質の陽性率は奏効/安定群に比して進行群で高い傾向を示した($p = 0.0601$)。

考察

Gal-3 タンパク質の発現は腫瘍細胞においては、プラチナ製剤による治療で奏効/安定群に比して非奏効群(進行群)で高い陽性率を示し、さらに進行群で血中自己抗体量が高いことと、過去の報告から肺腺癌組織においてもプラチナ製剤耐性に関与していることが示唆される。さらに、肺腺癌患者の抗 Gal-3 自己抗体量を測定することで、プラチナ製剤の治療感受性予測が治療前の血清で容易に行える可能性を今回初めて明らかにした。

以上の結果から、肺腺癌患者の治療前血清中の抗 Gal-3 自己抗体検査はプラチナ製剤による治療後に進行する患者を事前に鑑別できる可能性が示唆され、このような患者は非プラチナ製剤を用いた治療に変更するなどの治療方針の変更に役立つ可能性がある。

Content

	Page
1. Introduction	1
2. Materials and Methods	
2-1. Cell lines	3
2-2. Serum and tissue samples	3
2-3. Two-dimensional gel electrophoresis-immunoblotting	3
2-4. Identification of proteins recognized by autoantibodies	4
2-5. One-dimensional gel electrophoresis immunoblotting	5
2-6. Immunohistochemistry	5
2-7. Evaluation of immunohistochemistry	6
2-8. Preparation of Gal-3 protein for dot-blot analysis	6
2-9. Dot blot analysis	6
3. Results	
3-1. Autoantigens identified by 2DE-IB	8
3-2. Gal-3 expression in lung cancer cell lines	8
3-3. Extraction of Gal-3 protein using electro-elution method	8
3-4. Different reactivity of anti-Gal-3 autoantibody to recombinant or extracted Gal-3 proteins	8
3-5. Validation of anti-Gal-3 autoantibody	8
3-6. Gal-3 expression in lung cancer biopsy samples	9
4. Discussion	10
5. Abstract	12
6. Acknowledgements	13
7. References	14
8. Figure and Table	16

1. Introduction

Lung cancer is one of the most common neoplasms worldwide. It is the leading cause of cancer-related death in Japan, and the 5-year overall survival rate is still below 16%. Non-small cell lung cancer (NSCLC) accounts for approximately 80% of all lung cancers, and adenocarcinoma (AC) comprises about 50% of NSCLC (Jemal et al., 2007). Although platinum-based chemotherapy regimens improve the survival of patients with advanced NSCLC, resistance to chemotherapeutic agents is a major problem (Watanabe et al., 2003, Perng et al., 2008). In clinical practice, the chemotherapy response is variable among individuals. About one-third of NSCLC patients achieve complete remission (CR) or a partial response (PR) following the standard first-line chemotherapy, while another one-third show stable disease (SD) and progressive disease (PD), respectively (Chang, 2011). Thus, the identification of predictive markers of the response to chemotherapy is an urgent issue.

Autoantibodies are generally produced in sera of patients with various autoimmune diseases. They are also frequently observed in sera of patients with various neoplasms, even in the early stages. Therefore, the possibilities of using them as potential tumor markers have been suggested (Naour et al., 2002; Fernández-Madrid et al., 2004; Xia et al., 2005). Hanash (Hanash, 2003) reported that analyzing the immune response to identify novel cancer biomarkers is an attractive strategy, because the immune system induces biological amplification that is equivalent to a polymerase chain reaction (PCR) by generating a detectable signal with antigenic tumor proteins as templates, beginning at a very early stage during tumor development before the tumor is identifiable. Some tumor-associated autoantibodies have also been reported for lung cancer (Vural et al., 2005; Yagihashi et al., 2005). Cis-diamino-dichloroplatinum (II) (cisplatin) is a common agent used for chemotherapy against various cancers, including lung cancer. Cisplatin is a cytotoxic compound, which inhibits transcription and DNA replication, and induces apoptosis (Gonzalez et al., 2001). For lung cancer patients, cisplatin was found to be more effective than radiotherapy, and the combination of cisplatin and vinorelbine improved survival (Pepe et al., 2007). Multiple mechanisms have been suggested to explain platinum resistance, such as decreased tumor blood flow, altered extracellular conditions, reduced platinum uptake, increased efflux, intracellular detoxification by glutathione or decreased binding, DNA repair, decreased mismatch repair, defective apoptosis, the activation of anti-apoptotic factors or other signaling pathways, or the presence of quiescent non-cycling cells (Stewart, 2007). The mechanisms underlying cisplatin resistance have not been fully elucidated, and response-predictive markers of cisplatin have not been identified, which are clinical issues.

In this study, we searched for novel predictive markers of the therapeutic effect of cisplatin by two-dimensional immunoblotting (2DE-IB) with pretreated sera from patients who showed a partial response (PR) or progressive disease (PD) after platinum-based chemotherapy, and found that anti-Galectin-3 (Gal-3) autoantibody was correlated with the efficacy of the response to platinumbased chemotherapy.

2. Materials and Methods

2-1. Cell lines

The LC2/ad cell line derived from lung AC was purchased from RIKEN BioResource Center (Ibaraki, Japan). LC2/ad cells were grown in RPMI-1640 medium (SIGMA, Steinheim, Germany) supplemented with 10% heat-inactivated fetal bovine serum (Biowest, Miami, FL, USA), 100 units/mL penicillin, and 100 µg/mL streptomycin (Life Technologies Corp., Carlsbad, CA, USA). Cells were kept at 37°C in a humidified atmosphere of 5% CO₂ and 95% air. Harvested cells were washed twice with phosphate-buffered saline without bivalent ions (PBS-) and stored at -80°C. A cisplatin-resistant sub-line (LC2/ad-cis) was previously established and stably grown with a concentration of 3,200 ng/mL cisplatin for over 12 months in our laboratory (Kageyama et al., 2011). After harvesting and washing twice with PBS-, LC2/ad-cis cells were stored at -80°C.

2-2. Serum and tissue samples

The pre-treated sera from 22 patients with lung AC, who received platinum-based chemotherapy at Kitasato University Hospital, were collected and stored at -80°C until use. The number of underwent platinum-based chemotherapy and responses are shown in Table 1. Eight patients received cisplatin-based chemotherapy, including gemcitabine for 7 patients and docetaxel for the remaining one. Fourteen patients were treated with carboplatin-based chemotherapy, including 3 with gemcitabine, 2 with docetaxel, and 9 with paclitaxel. The responses to the chemotherapies were assessed by RECIST (version 1.1), and as shown in Table 1, 7 patients showed PR, 6 showed SD, and 9 showed PD. Pre-treatment biopsy samples from 40 lung AC patients who received platinum-based chemotherapy, at Kitasato University Hospital were used in this study. Among the 40 patients, 30 were treated with cisplatin-based regimens including 22 with gemcitabine, 7 with irinotecan, and 1 with etoposide. The remaining 10 patients were treated with carboplatin-based chemotherapy: 8 with paclitaxel and 2 with etoposide. The responses to the chemotherapies were assessed as PR in 11, SD in 14, and PD in 15 patients. All samples were collected in accordance with the ethical guidelines and written consent mandated, and this study was approved by the Ethics Committee of Kitasato University School of Medicine (B07-06). All patients were approached based on approved ethical guidelines, and all agreed to participate in this study and provided written consent. Patients could refuse entry and discontinue participation at any time.

2-3. Two-dimensional gel electrophoresis-immunoblotting

Two-dimensional gel electrophoresis with agarose (agarose 2-DE) method was performed with minor modifications to make it suitable for mini-gel (Nagashio et al., 2008). In brief, LC2/ad-cis cells were solubilized in lysis buffer [7 M urea, 2 M thiourea, 2% 3-[(3-cholamidopropyl) dimethylammonio] propanesulfonic acid, 0.1 M dithiothreitol, 2.5% pH 3-10 Pharmalyte (GE Healthcare Bio-Sciences, Piscataway, NJ, USA), and 0.1 tablet/mL of complete mini EDTA-free protease inhibitors (Roche Diagnostics, Mannheim, Germany)] using an ultrasonic homogenizer (VP-050; TAITEC, Saitama, Japan), and centrifuged at 20,000 x g for 30 min at 4°C. The protein was performed using 2-D Clean-Up Kit (GE Healthcare). The first-dimensional agarose isoelectric focusing (IEF) gel (80 mm long, 2.5-mm inner diameter) was made using a single pH 3-10 pharmalyte. The extracted proteins were applied to the cathodic end of the agarose IEF gel, and loaded at 4°C in stepwise voltages (1 hr at 100 V, 1 hr at 300 V, 1 hr at 500 V, 2 hrs at 700 V, and 3 hrs at 900 V). Then, the gels were immersed in trichloroacetic acid (TCA)-fixative solution (10% trichloroacetic acid, 5% sulfosalicylic acid) for 3 min at room temperature (RT) with shaking. After rinsing in distilled water (DW) three times for 15 min each, gels were treated in sodium dodecylsulfate (SDS) solutions (0.05 M Tris-HCl pH 6.8, 2% sodium dodecyl sulfate, 10% glycerol, 5% mercaptoethanol, and 0.02% bromophenol blue) for 15 min at RT with mild shaking. Then, each agarose gel was placed on the top of the second dimensional SDS-polyacrylamide gel electrophoresis (SDS-PAGE) gel with 12% polyacrylamide gel (7-9 cm), and loaded with a constant current at 20 mA. Two pieces of gel were prepared: one was for protein transfer to a polyvinylidene difluoride membrane (Millipore, Bedford, MA, USA) for immunoblotting, and the other was stained with coomassie brilliant blue R-350 (CBB) solution (PhastGel Blue R; GE Healthcare). After blocking with 0.5% casein/0.01 M Tris-HCl, pH 7.5, 150 mM NaCl (TBS) for 60 min at RT, the membranes were reacted with 100-times-diluted pre-treated sera from three lung AC patients who were assessed as showing PR or PD after platinum-based chemotherapy with 0.5% casein/TBS-T (TBS containing 0.1% Tween20) overnight at RT. Then, the membranes were reacted with 1,000-times-diluted horseradish peroxidase (HRP)- conjugated rabbit anti-human IgG polyclonal antibody (Dako, Glostrup, Denmark) with 0.5% casein/TBS-T for 30 min at RT. Finally, immunoreactive spots on the membranes were visualized with the Stable DAB solution (Lifetechnologies Corp.).

2-4. Identification of proteins recognized by autoantibodies

The protein spots matched with the immunoreactive spots were manually excised from CBB-stained 2-DE gels and destained with 50% acetonitrile (ACN)/50 mM NH₄HCO₃. The pieces of gel were dehydrated with 100% ACN and dried under vacuum conditions. Continuously, they were rehydrated in 10 µL of digestion solution containing 10 ng/µL trypsin (Trypsin Gold, Mass Spectrometry Grade, Promega, Madison, WI, USA) for 45 min at 4°C, and then incubated for 24 hrs at 37°C with a minimum volume of 25 mM NH₄HCO₃. After incubation, digested tryptic peptide solutions were collected, and the gel was washed once with 50% ACN/5% trifluoroacetic acid and collected in the same tube. Solutions containing digested tryptic peptide were then subjected to peptide mass fingerprint (PMF) and MS/MS analyses for protein identification with autoflex III matrix assisted laser desorption ionization-time of flight/ time of flight mass spectrometry (MALDI-TOF/TOF MS, Bruker Daltonics GmbH, Bremen, Germany). The PMF and MS/MS spectra were submitted to MASCOT ([http:// www.matrixscience.com/](http://www.matrixscience.com/)) for a database search, and the identification of corresponding proteins was conducted with the following database: IPI human database version 3.85 (89,952 sequences; 36,291,020 residues, <http://www.ebi.ac.uk/IPI/IPIhuman.>).

2-5. One-dimensional gel electrophoresis immunoblotting

Proteins were extracted from lung cancer cell lines with detergent lysis buffer (Laemmli, 1970) using an ultra-sonic homogenizer (VP-050; TAITTEC). Each 10 µg of extracted proteins was boiled and separated by SDS-PAGE using 10% gel with a constant current at 20 mA. After being transferred onto a PVDF membrane and blocked with 0.5% casein/TBS-T for 60 min at RT, the membranes were reacted with 500-times-diluted antiGal-3 antibody (Leica Biosystems, Milton Keynes, UK) with 0.5% casein/TBS-T for 2 hrs at RT. The membranes were continuously reacted with 1,000-times-diluted HRPconjugated rabbit anti-mouse IgG polyclonal antibody (Dako) with 0.5% casein/TBS for 30 min at RT. Finally, immunoreactive bands on the membranes were detected with Chemiluminescent HRP Substrate (Millipore Corp.), and captured with ATTO Cool Saver System (ATTO, Tokyo, Japan).

2-6. Immunohistochemistry

Ten percent formalin-fixed and paraffin-embedded lung cancer cell lines and lung AC biopsy specimens were used for IHC. Three-micrometer-thick sections were deparaffinized in xylene and rehydrated in a descending ethanol series, and then treated with 3% hydrogen peroxide for

10 min. After blocking with 2% normal swine serum (NSS)/TBS for 10 min at RT, the sections were reacted with 200-times-diluted anti-Gal-3 antibody with 2% NSS/TBS for 16-18 hrs at RT. Then, the sections were reacted with ChemMate ENVISION reagent (Dako) for 30 min at RT. Finally, the sections were visualized using Stable DAB solution (Invitrogen) and counterstained with Mayer's hematoxylin.

2-7. Evaluation of immunohistochemistry

Cytoplasmic immunostaining of tumor cells was considered to be a positive result for anti-Gal-3 autoantibody. The staining intensity was categorized into four groups: 0=negative; 1=weakly positive; 2=moderately positive, 3=strongly positive. The tumor cells with staining scores of 2 and 3 were judged as positive. The χ^2 -test was used for the statistical evaluation of staining data. $p < 0.05$ was considered significant.

2-8. Preparation of Gal-3 protein for dot-blot analysis

i) Electro-elution method

Protein extraction from the CBB-stained 2-DE gels were performed using Mini GeBA (Gene Bio-Application Ltd., Yavne, Israel) according to the manufacturer's instructions. In brief, a Gal-3 protein spot was excised from 2-DE gel and transferred to a Mini GeBAflex-tube. After being filled with proteinrunning buffer (0.192 M glycine, 0.025 M Tris-HCl pH 7.5, and 0.1% SDS) and placed in the supporting tray, the tube was loaded at 100 V until the protein exited the gel slice using a mini-gel electrophoresis chamber (Mupid, ADVANCE CO., Ltd., Saitama, Japan). Next, reversing the polarity of the electric current for 120 sec, the protein-containing solution was transferred to a clean tube. Then, an equal volume of 20% TCA was added to the tube and it was incubated for 1 hr at 4°C, centrifuged at 18,000 x g for 30 min at 4°C, and the supernatant was discarded. After adding cold acetone, the sample was incubated at -20°C for 1 hr, and then centrifuged at 18,000 x g for 30 min at 4°C. Finally, the supernatant was discarded, the pellet was air-dried, and Gal-3 protein was solubilized with detergent lysis buffer using an ultra-sonic homogenizer.

ii)Recombinant Gal-3 protein

Recombinant Gal-3 protein was prepared using a wheat germ cell-free system (Goshima et al., 2008). Protein information and the sequence ID of recombinant Gal-3 protein are FLJ95838AAAF and G-BRTHA2025858_F.1, respectively (<http://hgpd.lifesciencedb.jp/cgi/index.cgi>).

2-9. Dot blot analysis

IgG levels of anti-Gal-3 autoantibody in sera were detected employing the automatic dot blot system, with a 256-solid pin configuration (Kakengeneqs Co., Ltd., Chiba, Japan). Gal-3 protein extracted by the electroelution method and recombinant protein were spotted onto the PVDF membranes. After being washed in TBS, the membranes were blocked with 2% Tween 20 in TBS for 1 hr at RT. Then, the membranes were reacted with 1,000-times-diluted pre-treated sera with TBS-T for 16- 18 hrs at 4°C. After washing 3 times for 5 min each in TBS-T, the membranes were incubated with 1,000-timesdiluted HRP-conjugated rabbit anti-human IgG polyclonal antibody (Dako) for 30 min at RT. Finally, signals were developed with Immobilon Western reagent (Millipore Corp.). The data were analyzed using DotBlotChipSystem software ver. 4.0 (Dynacom Co., Ltd., Chiba, Japan). Normalized signals are presented as the positive intensity minus background intensity around the spot. Statistical analysis was performed using the Mann-Whitney U-test. The area under the curve (AUC) and best cut-off point were calculated by employing receiver operating characteristics (ROC) analysis.

3. Results

3-1. Autoantigens identified by 2DE-IB

The proteins extracted from LC2/ad-cis cells were separated by 2-DE, transferred onto a PVDF membrane, and reacted with pre-treated sera from three patients who were assessed as showing PD or PR after platinum-based chemotherapy (Figure 1). Ninety-five and 63 immunoreactive spots were detected with pre-treated sera from AC patients who showed PD and PR, respectively. In total, 51 proteins including Gal-3 in PD and 12 proteins in PR patients, respectively, were identified (Table 2).

3-2. Gal-3 expression in lung cancer cell lines

To confirm whether Gal-3 was over-expressed in LC2/ad-cis cells compared to that in LC2/ad cells, we performed IB and IHC analysis using freshly frozen and formalin-fixed and paraffin-embedded LC2/ad cells and LC2/ad-cis cells, respectively (Figure 2). We confirmed that the expression of Gal-3 up-regulated in LC2/ad-cis cells and that positive staining was observed in the cytoplasm.

3-3. Extraction of Gal-3 protein using electro-elution method

We extracted Gal-3 protein from 2DE gels by the electro-elution method. The reactivity of extracted Gal-3 protein was confirmed by immunoblot analysis (Figure 3).

3-4. Different reactivity of anti-Gal-3 autoantibody to recombinant or extracted Gal-3 proteins

Anti-Gal-3 autoantibody in pre-treated sera from lung AC patients did not react with recombinant Gal-3 protein, but showed strong reactivity with Gal-3 protein extracted from tumor cells (Figure 4). Thus, the serum IgG levels of anti-Gal-3 autoantibody were validated by the dot blot analysis with extracted Gal-3 protein from tumor cells.

3-5. Validation of anti-Gal-3 autoantibody

To confirm its utility as a potential predictive biomarker of the efficacy of platinum-based chemotherapy against lung AC, we investigated IgG levels of anti-Gal-3 autoantibody in pre-treated sera by dot-blot analysis. The serum IgG levels of anti-Gal-3 autoantibody in PR, PD, and SD groups ranged from 190 to 1,070 (median: 550), 650 to 2,300 (median: 1,140), and 310 to 1,150 (median: 880), respectively. The serum IgG levels of anti-Gal-3 autoantibody were significantly higher in the PD group than in PR and SD groups ($p=0.0084$) (Figure 4 and Figure

5 A). An optimal cut-off value of 1,086 was applied based on ROC analysis, and the predictive sensitivity and specificity for platinum-based chemotherapy was 67 and 92%, respectively (Figure 5 B). The AUC for anti-Gal-3 autoantibody in patients who showed PD compared to SD and PR after platinum-based chemotherapy was 0.84.

3-6. Gal-3 expression in lung cancer biopsy samples

To further clarify the relation between Gal-3 expression and the efficacy of platinum-based chemotherapy, we compared the stainability and clinical data in 40 pretreated lung biopsy samples. We judged the Gal-3 staining as positive when the staining score was 2 or 3 (Figure 6 A), while it was negative when the score was 0 or 1 (Figure 6 B). Gal-3 expression was evaluated as positive in 10 of 15 (66.7%) PD, 7 of 14 (50.0%) SD, and in 2 of 11 (18.2%) PR patients, respectively. The positive rate of Gal-3 was in the order of PD, SD, and PR groups ($p=0.0601$).

4. Discussion

In the present study, to identify novel biomarkers that can predict the efficacy of platinum-based chemotherapy, we performed 2DE-IB to detect autoantigens that are recognized by autoantibodies in pre-treated sera from lung AC patients assessed as showing PD or PR after platinum-based chemotherapy. Sixty-three autoantigens in total were identified by 2DE-IB.

We focused on Gal-3 from the identified candidate autoantigens, because it was reported that intracellular Gal-3 exhibits activity to suppress drug-induced apoptosis, which was reported to be essential for cancer cell survival and tumor progression in various tumor types (Tsuboi et al., 2007, Park et al., 2008, Saussez et al., 2008, Chiu et al., 2010) and Gal-3 thus has been proposed as an antiapoptotic factor in response to chemotherapeutic drugs, and its down-regulation could improve the efficacy of anticancer drugs (Fukumori et al., 2006). However, to our knowledge, there has been no study on the utility of Gal-3 as an anti-apoptotic factor in lung cancer. They also reported that the expression of Gal-3 protein stimulated the phosphorylation of Ser112 of Bcl-2-associated death (Bad) protein and down-regulated Bad expression after treatment with cisplatin. And, Gal-3 also inhibited mitochondrial depolarization and damage after translocation from the nuclei to cytoplasm, resulting in the inhibition of cytochrome c release and caspase-3 activation (Fukumori et al., 2006). These study suggest that Gal-3 inhibits drug-induced apoptosis through the phosphorylation of Bad protein and suppression of the mitochondrial apoptosis pathway.

Cisplatin-induced apoptosis was increased after knocking down the expression of Gal-3, and this cytotoxic effect was canceled by roscovitine, an inhibitor of cyclin-dependent protein kinase (Oishi et al., 2007). Wongkham et al. (Wongkham et al., 2009) reported that the cellular levels of Gal-3 might contribute to the anti-apoptotic activity and chemoresistance of cholangiocarcinoma cells. In the present study, the expression of Gal-3 was up-regulated in cisplatin-resistant LC2/ad-cis cells compared with the parental LC2/ad cells, consistent with previous reports (Fukumori et al., 2006, Oishi et al., 2007). Although the expression levels of Gal-3 in tumor cells have been reported to be correlated with cisplatin resistance, the association between serum IgG levels of anti-Gal-3 autoantibody and cisplatin resistance has not been investigated.

To confirm the possibility of using anti-Gal-3 autoantibody as a novel predictive marker of the efficacy of platinum-based chemotherapy, we measured the serum anti-Gal-3 autoantibody levels in patients with diseases assessed as showing PR, SD, or PD following platinum-based treatment by dot-blot analysis. We demonstrated that the serum anti-Gal-3 autoantibody levels were significantly higher in the PD group than in PR and SD groups ($p=0.0084$). Furthermore, IHC

staining of pretreated lung biopsy samples also showed that the positive rate of Gal-3 was highest in the PD group, and was decreased in the order of PD, SD, and PR groups ($p=0.052$). Our results confirmed that the expression of Gal-3 had a role in the anti-apoptotic activity and chemoresistance. Taken together, our results suggest the serum anti-Gal-3 autoantibody levels might be a useful predictive marker of the efficacy of platinum-based chemotherapy.

The different reactivity between recombinant and extracted Gal-3 proteins might be caused by the presence or absence of post-translational modifications (PTM) (Balan et al., 2010). The present data raise the possibility that anti-Gal-3 autoantibody in sera from lung AC patients reacts with the modification-received Gal-3 protein, and further studies are necessary to investigate this hypothesis.

In conclusion, we demonstrated that IgG levels of antiGal-3 autoantibody in pre-treated sera were significantly higher in patients assessed as showing PD than as PR and SD after platinum-based chemotherapy. Our data suggest that the IgG levels of anti-Gal-3 autoantibody provide a novel predictive biomarker of the efficacy of platinumbased chemotherapy.

5. Abstract

Background: Identification of predictive markers for the efficacy of platinum-based chemotherapy is necessary to improve the quality of the life of cancer patients.

Materials and Methods: We detected proteins recognized by autoantibodies in pretreated sera from patients with lung adenocarcinoma (AC) evaluated as showing progressive disease (PD) or a partial response (PR) after cisplatin-based chemotherapy by proteomic analysis. Then, the levels of the candidate autoantibodies in the pretreated serum were validated by dot-blot analysis for 22 AC patients who received platinum-based chemotherapy, and the expression of identified proteins was immunohistochemically analyzed in 40 AC biopsy specimens.

Results: An autoantibody against galectin-3 (Gal-3) was detected in pretreated sera from an AC patient with PD. Serum IgG levels of anti-Gal-3 autoantibody were significantly higher in patients evaluated with PD than in those with PR and stable disease (SD) ($p = 0.0084$). Furthermore, pretreated biopsy specimens taken from patients evaluated as showing PD following platinum-based chemotherapy showed a tendency to have a higher positive rate of Gal-3 than those with PR and SD ($p = 0.0601$).

Conclusions: These results suggest that serum IgG levels of anti-Gal-3 autoantibody may be useful to predict the efficacy of platinum-based chemotherapy for patients with lung AC

6. Acknowledgements

This study was supported in part by JSPS KAKENHI Grant Number 23590414, the JST-SENTAN (Development of Systems and Technology for Advanced Measurement and Analysis: Life Innovation Area) program from the Japan Science and Technology Agency, the Japan Society for the Promotion of Science fellows (25-5519), the 2013-2014 Project Study from the Graduate School of Medical Sciences, the Research Project (No. 2013-1004) from the School of Allied Health Sciences, Kitasato University, and a grant-in-aid of The Ishitsu Shun Memorial Scholarship, Japan.

7. References

- Balan V, Nangia-Makker P, Jung YS, et al (2010). Galectin-3: a novel substrate for c-Abl kinase. *Biochem Biophys Acta*, 1803, 1198-205.
- Chang A (2011). Chemotherapy, chemoresistance and the changing treatment landscape for NSCLC. *Lung Cancer*, 7, 3-10.
- Chiu CG, Strugnelli SS, Griffith OL, et al. Diagnostic utility of galectin-3 in thyroid cancer. *Am J Pathol*, 176, 2067-81.
- Fernández-Madrid F, Tang N, Alansari H, et al (2004). Autoantibodies to Annexin XI-A and other autoantigens in the diagnosis of breast cancer. *Cancer Res*, 64, 5089-96.
- Fukumori T, Oka N, Takenaka Y, et al. Galectin-3 regulates mitochondrial stability and antiapoptotic function in response to anticancer drug in prostate cancer. *Cancer Res*, 66, 3114-9.
- Gonzalez V M, Fuertes M A, Alonso C, et al (2001). Is cisplatin-induced cell death always produced by apoptosis? *Mol Pharmacol*, 59, 657-63.
- Goshima N, Kawamura Y, Fukumoto A, et al. Human protein factory for converting the transcriptome into an in vitro expressed proteome. *Nat Methods*, 5, 1011-7.
- Hanash S (2003). Harnessing immunity for cancer marker discovery. *Nat Biotechnol*, 21, 37-8.
- Jemal A, Siegel R, Ward E, et al (2007). Cancer statistics, 2007. *CA Cancer J Clin*, 57, 43-66.
- Kageyama T, Nagashio R, Ryuge S, et al (2011). HADHA is a potential predictor of response to platinum-based chemotherapy for lung cancer. *Asian Pac J Cancer Prev*, 12, 3457-63.
- Laemmli UK (1970). Cleavage of structural proteins during the assembly of the head of bacteriophage T4. *Nature*, 227, 680-5.
- Le Naour F, Brichory F, Misek DE, et al (2002). A distinct repertoire of autoantibodies in hepatocellular carcinoma identified by proteomic analysis. *Mol Cell Proteomics*, 1, 197-203.
- Nagashio R, Sato Y, Jiang SX, et al (2008). Detection of tumorspecific autoantibodies in sera of patients with lung cancer. *Lung Cancer*, 62, 364-73.
- Oishi T, Itamochi H, Kigawa J, et al (2007). Galectin-3 may contribute to Cisplatin resistance in clear cell carcinoma of the ovary. *Int J Gynecol Cancer*, 17, 1040-6.
- Park SH, Min HS, Kim B, et al (2008). Galectin-3: a useful biomarker for differential diagnosis of brain tumors. *Neuropathology*, 28, 497-506.
- Pepe C, Hasan B, Winton TL, et al (2007). Adjuvant vinorelbine and cisplatin in elderly patients: National Cancer Institute of Canada and Intergroup Study JBR.10. *J Clin Oncol*, 25, 1553-61.
- Perng RP, Yang CH, Chen YM, et al (2008). High efficacy of erlotinib in Taiwanese NSCLC patients in an expanded access program study previously treated with chemotherapy. *Lung*

Cancer, 62, 78-84.

Saussez S, Decaestecker C, Mahillon V, et al (2008). Galectin-3 up-regulation during tumor progression in head and neck cancer. *Laryngoscope*, 118, 1583-90.

Stewart DJ (2007). Mechanism of resistance to cisplatin and carboplatin. *Crit Rev Oncol Hematol*, 63, 12-31.

Tsuboi K, Shimura T, Masuda N, et al (2007). Galectin-3 expression in colorectal cancer: relation to invasion and metastasis. *Anticancer Res*, 27, 2289-96.

Vural B, Chen LC, Saip P, et al (2005). Frequency of SOX Group B (SOX1, 2, 3) and ZIC2 antibodies in Turkish patients with small cell lung carcinoma and their correlation with clinical parameters. *Cancer*, 103, 2575-83.

Watanabe H, Yamamoto S, Kunitoh H, et al (2003). Tumor response to chemotherapy: the validity and reproducibility of RECIST guidelines in NSCLC patients. *Cancer Sci*, 94, 1015-20.

Wongkham S, Junking M, Wongkham C, et al (2009). Suppression of galectin-3 expression enhances apoptosis and chemosensitivity in liver fluke-associated cholangiocarcinoma. *Cancer Sci*, 100, 2077-84.

Xia Q, Kong XT, Zhang GA, et al (2005). Proteomics-based identification of DEAD-box protein 48 as a novel autoantigen, a prospective serum marker for pancreatic cancer. *Biochem Biophys Res Commun*, Kengo Yanagita et al 7966 *Asian Pacific Journal of Cancer Prevention*, Vol 16, 2015 330, 26-32.

Yagihashi A, Asanuma K, Kobayashi D, et al (2005). Detection of autoantibodies to livin and survivin in Sera from lung cancer patients. *Lung Cancer*, 48, 217-21.

8. Figure and Table

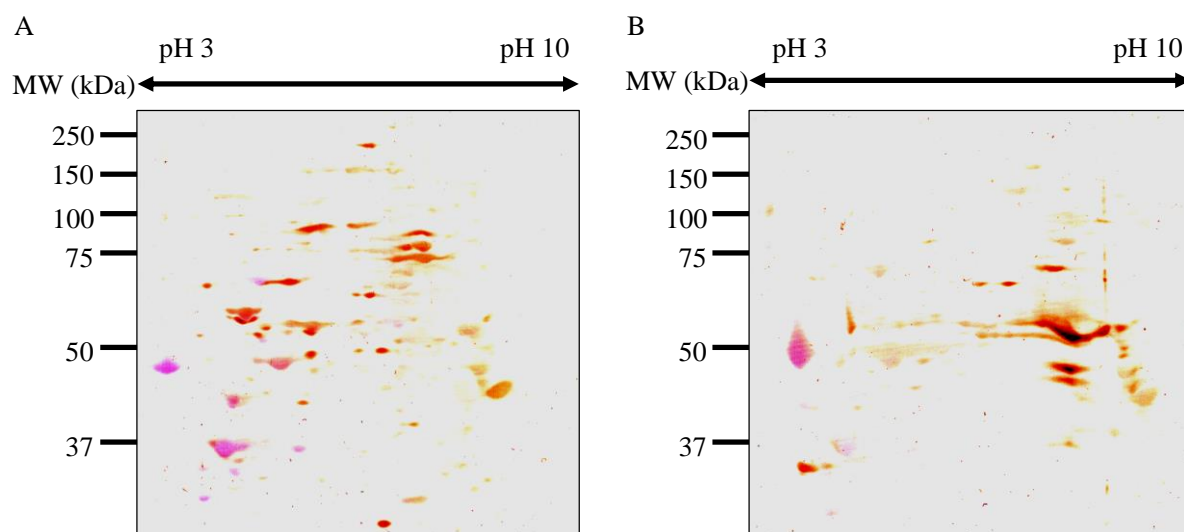


Figure 1. Detection of Autoantibodies in Pre-treated Sera from AC Patients who were Treated with Platinum-based Chemotherapy by 2DE-IB Analysis. Proteins extracted from LC2/ad-cis cells were separated by 2DE. Immunoblot analysis was performed with mixed pre-treated sera from AC patients assessed as showing PD (A) or PR (B) as a first-antibody, and the reaction was visualized with DAB solution.

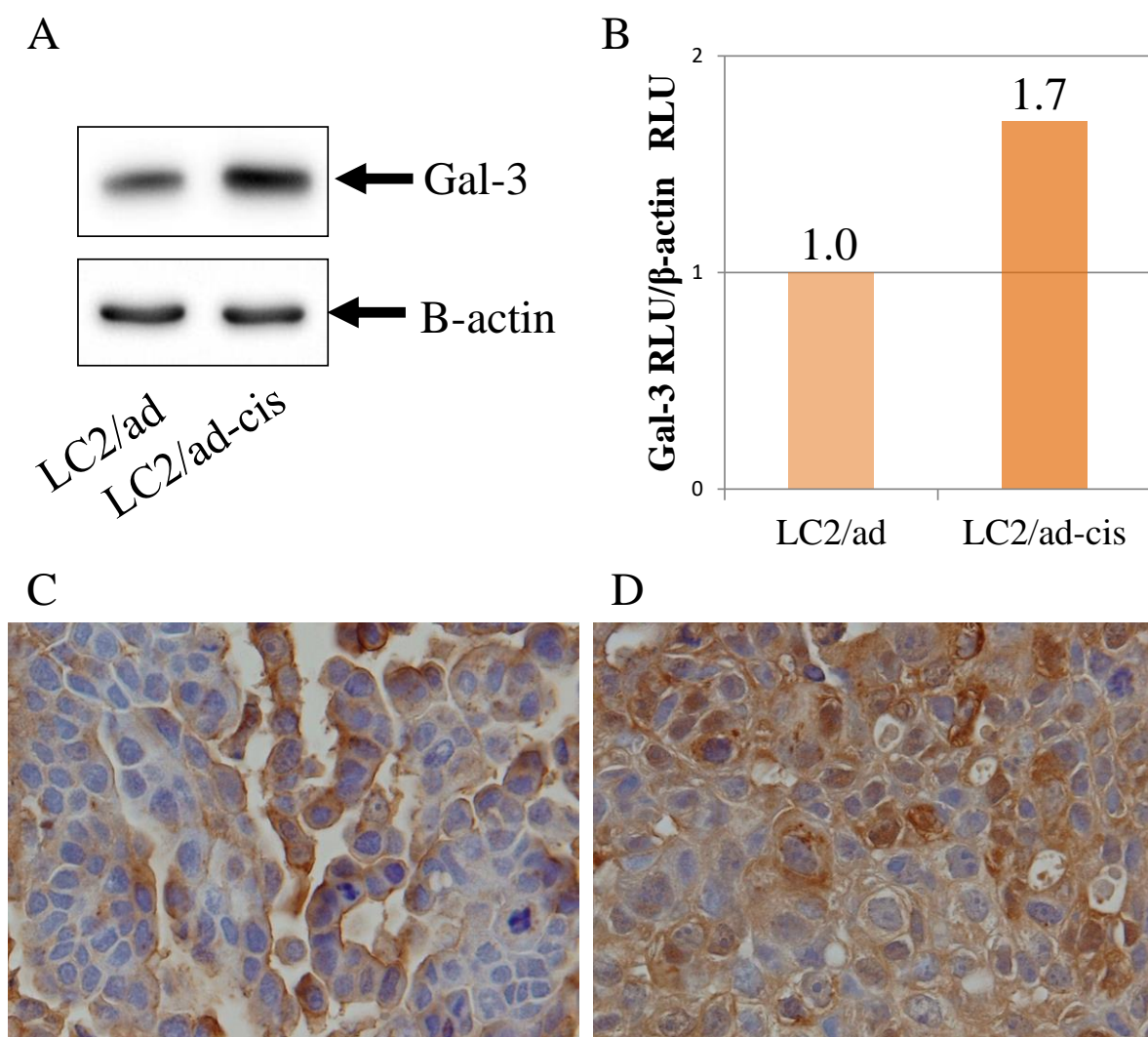


Figure 2. The Expression of Gal-3 in Cisplatin- Resistant LC2/ad-cis Cells and Sensitive LC2/ad Cells. (A) Expression levels of Gal-3 protein were detected by immunoblot analysis. Beta-actin was used as an internal control. (B) Expression levels of Gal-3 were normalized by expression levels of beta-actin and presented as Relative Light Units (RLU). Cytoplasmic staining of Gal-3 in LC2/ad cells (C) and LC2/ad-cis cells (D).

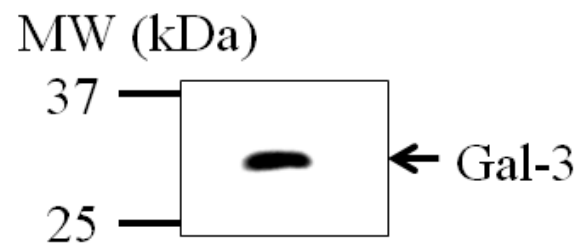


Figure 3. Gal-3 protein extracted from 2DE gels was confirmed by immunoblotting with anti-Gal-3 antibody.

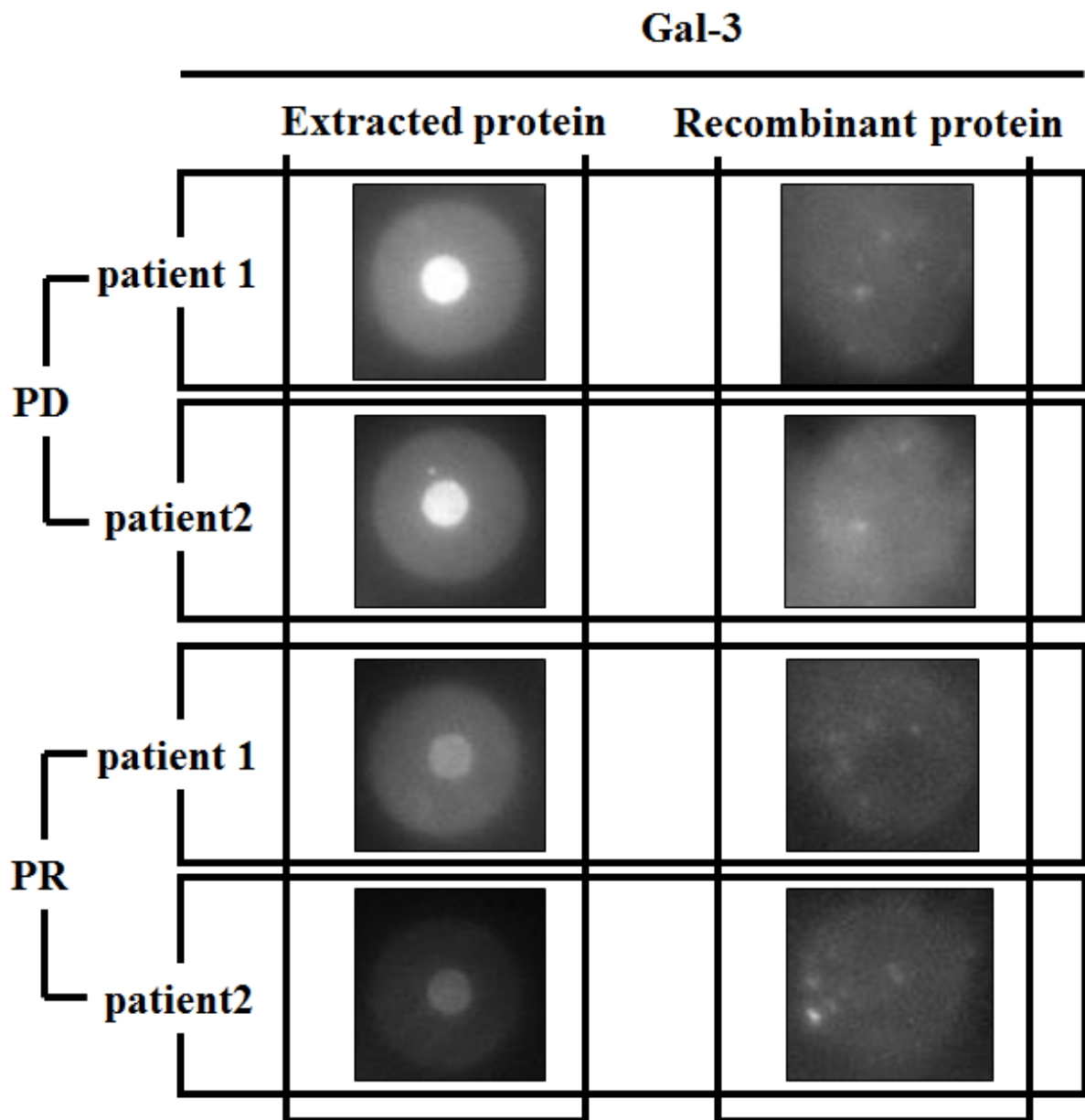


Figure 4. The reactivity of anti-Gal-3 autoantibody to recombinant or extracted Gal-3 proteins by dot-blot analysis. Extracted proteins using the electro-elution method or recombinant Gal-3 proteins were spotted onto PVDF membranes. The membranes were reacted with pretreated sera from AC patients showing PR or PD. For Gal-3 protein extracted from 2-DE gels, strong or weak signals of anti-Gal-3 autoantibody were detected in two each of AC patients diagnosed as showing PD or PR, respectively. However, no clear signals were detected with recombinant Gal-3 protein.

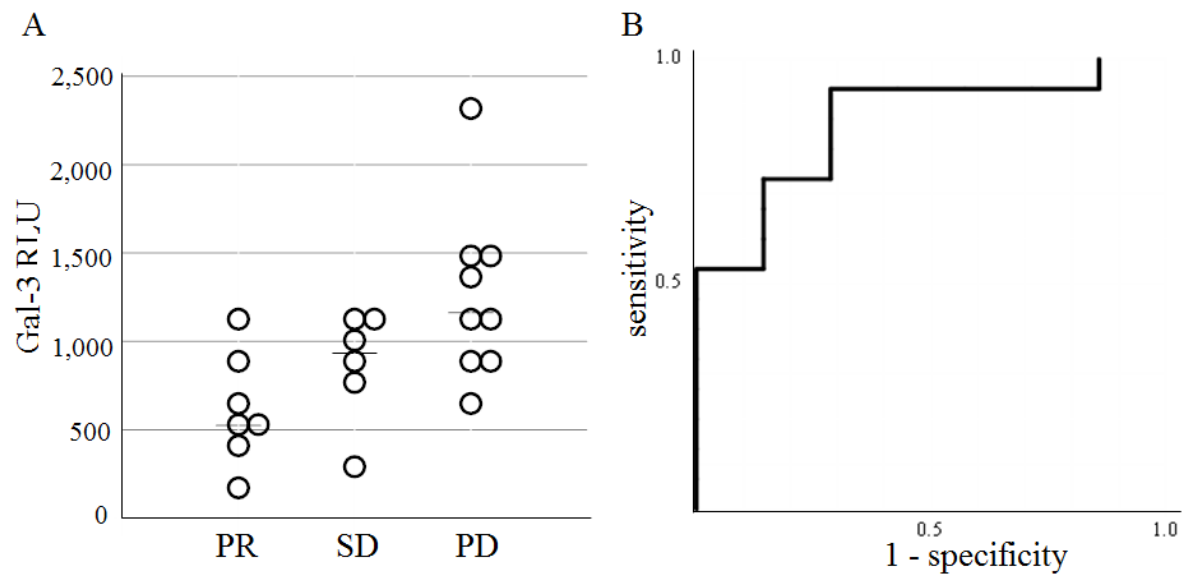


Figure 5. Anti-Gal-3 Autoantibody Levels in Pre-Treated Sera from Lung Cancer Patients by Dot-blot Analysis. (A) The median Gal-3 autoantibody level in pre-treated sera from patients assessed as showing PR and SD or PD was 873 or 1,140. Anti-Gal-3 autoantibody levels were significantly higher in PD patients than PR and SD patients ($p < 0.0084$). (B) Receiver operating characteristic curve (ROC) analysis of serum anti-Gal-3 autoantibody levels as a predictive marker of the efficacy of platinum-based chemotherapy against lung adenocarcinoma. The corresponding area under the curve was 0.84 for anti-Gal-3 autoantibody. With 92% specificity, the sensitivity of anti-Gal-3 autoantibody for patients assessed as showing PD was 67%, at a cut-off value corresponding to 1,086.

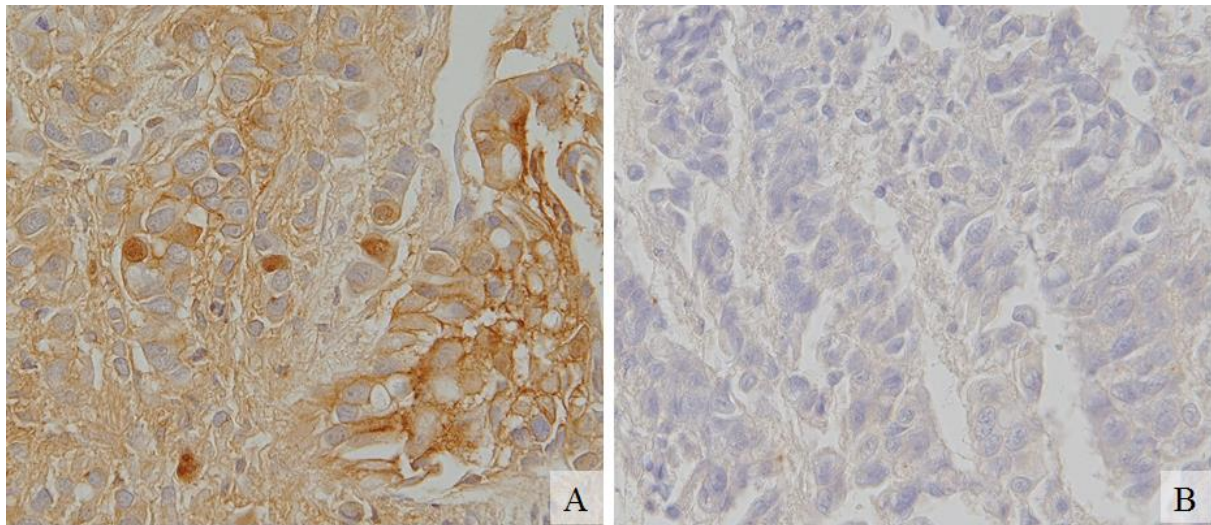


Figure 6. Expression of Gal-3 in lung cancer biopsy samples. (A) The section from patients who assessed as showing progressive disease (PD) following platinum-based chemotherapy was evaluated as Gal-3-positive. (B) The section from patients who assessed as showing partial response (PR) to platinum-based chemotherapy was evaluated as Gal-3-negative.

Table 1. Combinations of platinum-based chemotherapy in patients in this study

Regimen	n	Response		
		PR	SD	PD
CDDP + GEM	7	2	3	2
CDDP+DOC	1	1	0	0
CBDCA+GEM	3	0	0	3
CBDCA+DOC	2	0	1	1
CBDCA+PTX	9	4	2	3

CDDP, cisplatin; CBDCA, Carboplatin; GEM, gemcitabine; DOC, docetaxel; PTX, paclitaxel

	Gene symbol	Proteine name	IP1	Molecular weight (Da)	Function
PR	TUBA1A	tubulin, alpha 1a	00180675	50,136	The major constituent of microtubules
	KRT8	Keratin, type II cytoskeletal 8	00554648	53,704	helps to link the contractile apparatus to dystrophin at the costameres of striated muscle
	AHCY	Adenosylhomocysteinase	00012007	47,716	competitive inhibitor of S-adenosyl-L-methionine-dependent methyl transferase reactions
	LRMP	Lymphoid-restricted membrane protein 1	00006158	62,122	The protein encoded by this gene is expressed in a developmentally regulated manner in lymphoid cell lines and tissues.
	MYH4	Myosin-4	00001753	223,013	Muscle contraction
	LMNA	Prelamin-A/C		74,139	Accelerate smooth muscle cell senescence
	EEF1D	Eukaryotic translation elongation factor 1 delta	00023048	31,122	EF-1-beta and EF-1-delta stimulate the exchange of GDP bound to EF-1-alpha to GTP
	HNRNPA1	Heterogeneous nuclear ribonucleoprotein A1	00215965	34,196	Transport of poly(A) mRNA from the nucleus to the cytoplasm
	ACADM	Medium-chain specific acyl-CoA dehydrogenase, mitochondrial	00005040	44,892	This enzyme is specific for acyl chain lengths of 4 to 16
	SFPQ	Isoform Long of Splicing factor, proline-and glutamine-rich	00010740	76,149	DNA- and RNA binding protein, involved in several nuclear processes.
	DLST	Dihydrolipoylysine-residue succinyltransferase	00420108	48,755	Multiple copies of 3 enzymatic components
PD	TUBA1B	tubulin, alpha 1b	00792677	50,152	Tubulin is the major constituent of microtubules
	RDX	Radiixin	00017367	68,564	Crucial role in the binding of the barbed end of actin filaments to the plasma membrane
	EZR	Ezrin	00843975	69,413	Connections of major cytoskeletal structures to the plasma membrane
	HSP90AA1	Heat shock protein HSP 90-alpha	00784295	84,660	Molecular chaperone that promotes maturation
	KARS	Lysyl-tRNA synthetase	00014238	68,048	Catalyzes the specific attachment of an amino acid to its cognate tRNA in a 2 step reaction
	PDIA4	Protein disulfide isomerase family A, member 4	00009904	72,932	Catalyzes the rearrangement of -S-S- bonds in proteins
	TRAP1	TNF receptor-associated protein 1	00030275	80,110	Chaperone that expresses ATPase activity
	KRT19	Keratin, type I cytoskeletal 19	00794644	44,106	Involved in the organization of myofibers.
	HNRNPL	Heterogeneous nuclear ribonucleoprotein L	00027834	64,133	A component of the heterogeneous nuclear ribonucleoprotein (hnRNP) complexes
	KRT17	Keratin, type II cytoskeletal 7	00792841	51,386	Blocks interferon-dependent interphase and stimulates DNA synthesis in cells.
	KRT18	Keratin, type I cytoskeletal 18	00554788	48,058	Involved in the uptake of thrombin-antithrombin complexes by hepatic cells (By similarity).
	RUVBL2	RuvB-like 2	00009104	51,157	Possesses single-stranded DNA-stimulated ATPase and ATP-dependent DNA helicase (5' to 3') activity
	TUBB2C	Tubulin, beta 2c	00956734	49,831	Tubulin is the major constituent of microtubules
	TUBA1C	Tubulin, alpha 1c	00218343	49,895	Tubulin is the major constituent of microtubules
	SEPT11	Septin-11	00019376	49,398	Filament-forming cytoskeletal GTPase
	G6PD	Glucose-6-phosphate dehydrogenase	00884082	59,257	Produces pentose sugars
	EEF1A1	Elongation factor 1-alpha 1	00180730	50,141	This protein promotes the GTP-dependent binding of aminoacyl-tRNA to the A-site of ribosomes during protein biosynthesis
	IDH1	Isocitrate dehydrogenase cytoplasmic	00027223	46,659	Isocitrate dehydrogenases catalyze the oxidative decarboxylation of isocitrate to 2-oxoglutarate.
	PGAM1	Phosphoglycerate mutase 1	00549725	28,804	Interconversion of 3- and 2-phosphoglycerate with 2,3-bisphosphoglycerate as the primer of the reaction
	SLC25A5	ADP/ATP translocase 2	00007188	32,852	Catalyzes the exchange of ADP and ATP across the mitochondrial inner membrane
	PSMA1	Proteasome subunit alpha type-1	00910408	29,556	ATP-dependent proteolytic activity
	EFHD2	EF-hand domain-containing protein D2	00060181	26,697	Regulate B-cell receptor induced immature and primary B-cell apoptosis
	PHB	Prohibitin	00816719	29,804	Prohibitin inhibits DNA synthesis
	LDHB	L-lactate dehydrogenase B	00219217	36,638	This gene encodes an enzyme which catalyzes the reversible conversion of lactate and pyruvate, and NAD and NADH, in the glycolytic pathway.
	CAPZB	Isoform 2 of F-actin capping protein beta subunit	00642256	31,350	F-actin-capping proteins bind
	GALE	UDP-galactose-4-epimerase	00107100	38,282	Catalyzes two distinct but analogous reactions
	BUB3	Isoform 1 of mitotic checkpoint protein BUB 3	00013468	37,115	Has a dual function in spindle-assembly checkpoint signaling and in promoting the establishment of correct kinetochore-microtubule (K-MT) attachments.
	EIF2S1	Eukaryotic translation initiation factor 2, subunit 1	00219678	36,112	The early steps of protein synthesis by forming a ternary complex with GTP and initiator tRNA
	NOO1	NAD(P)H dehydrogenase 1	00619966	30,868	The vitamin K-dependent gamma-carboxylation of glutamate residues in prothrombin synthesis
	LGALS3	Galectin-3	00385850	26,152	Acute inflammatory responses including neutrophil activation and adhesion, chemoattraction of monocytes
	GNB2L1	Guanine nucleotide binding protein subunit beta 2	00848226	35,077	The recruitment, assembly and/or regulation of a variety of signaling molecules
	HNRNPA2B1	Heterogeneous nuclear ribonucleoprotein A2/B1	00414696	37,430	pre-mRNA processing
	GAPDH	Glyceraldehyde-3-phosphate dehydrogenase	00219018	36,053	Glyceraldehyde-3-phosphate dehydrogenase and nitrosylase activities
	ALDOA	Fructose-bisphosphate aldolase A	00465439	39,420	Glycolysis and gluconeogenesis
	PSMC6	26S protease regulatory subunit S10B	00910829	44,173	ATP-dependent degradation of ubiquitinated proteins
	FH	Fumarate hydratase	00759715	54,637	Acts as a tumor suppressor
	ENO1	Enolase 1	00465248	47,169	Multifunctional enzyme
	ANXA11	Annexin A11	00414320	54,390	Produces pentose sugars
	UGDH	UDP-glucose 6-dehydrogenase	00968010	55,024	Biosynthesis of glycosaminoglycans
	GSR	Isoform Mitochondrial of Glutathione reductase	00016862	56,257	Binds specifically to calyculin
	SHMT2	Serine hydroxymethyltransferase 2	00794572	55,993	Interconversion of serine and glycine
	CCT7	T-complex protein 1 subunit 7	00952607	59,367	Folding of proteins upon ATP hydrolysis
	DDX6	Probable ATP-dependent RNA helicase DDX6	00030320	54,417	mRNA decapping
	DDX5	Probable ATP-dependent RNA helicase DDX5	00017617	69,148	RNA-dependent ATPase activity
	OGG1	8-oxoguanine DNA glycosylase	01013811	38,782	DNA repair enzyme that incises DNA at 8-oxoG residues.
	AIFM1	Apoptosis-inducing factor 1	01015707	66,901	Controlling cellular life and death
	KRT10	Keratin, type I cytoskeletal 10	00009865	58,827	This gene encodes a member of the type I (acidic) cytokeratin family, which belongs to the superfamily of intermediate filament (IF) proteins.
	tmpo	Thymopoietin	00216230	75,492	Structural organization of the nucleus
	NCL	Nucleolin	00916991	76,614	Nucleolar protein of growing eukaryotic cells
	KHSRP	Far upstream element-binding protein	00855957	73,115	Dendritic targeting element
	UBA1	Ubiquitin-like modifier activating enzyme 1	00645078	117,849	Activates ubiquitin
	DDX1	Probable ATP-dependent RNA helicase DDX1	00293655	82,432	ATP-dependent RNA helicase

PR: partial response, PD: progressive disease